

# A Newly Developed Wrought Ni–Fe–Cr-based Superalloy for Advanced Ultra-Supercritical Power Plant Applications Beyond 700 °C

Shuai Guan<sup>1</sup> · Chuan-Yong Cui<sup>1</sup>

Received: 11 May 2015 / Revised: 25 June 2015 / Published online: 21 July 2015  
© The Chinese Society for Metals and Springer-Verlag Berlin Heidelberg 2015

**Abstract** Some existing wrought Ni–Cr–Co-based superalloys are being evaluated as the candidate materials for advanced ultra-supercritical power plant applications beyond 700 °C due to their high creep strength. But they are all prohibitively expensive due to the addition of Co, Mo and W. Here we developed a new Ni–Fe–Cr-based superalloy (named as HT700 alloy) with low cost and high strength. This paper reports the mechanical properties and fracture modes of HT700 alloy to support its high temperature applications and to understand prospective failure mechanism. Fractographic examinations indicate that the fracture modes shift with test condition change. In addition, the HT700 alloy has relatively stable microstructure at 750 °C. Compared with IN740 and GH2984 alloys, this new alloy has higher yield strength in the temperature range from room temperature to 800 °C. The creep life of this new alloy is much longer than that of the Ni–Fe-based superalloy GH2984. The results suggest that this new alloy is a promising material for advanced ultra-supercritical power plant applications beyond 700 °C.

**KEY WORDS:** Wrought Ni–Fe–Cr-based superalloy; Low cost; High strength; Fracture mode

## 1 Introduction

In the twenty-first century, the world faces the critical challenge of providing abundant and cheap electricity to meet the needs of growing global population while at the same time preserving environmental values [1]. But traditional methods of coal combustion emit environmental pollutants and CO<sub>2</sub> (approximately 10 billion tons per year) at high levels compared to other energy generation options [1–3]. Therefore, the requirements for higher efficiency, less energy consumption and reduced environmental impact are pushing fossil-fired power plants to advanced

ultra-supercritical (A-USC) conditions with steam temperature of up to 700–760 °C and pressure of up to 35–37.5 MPa [4–7]. The key to higher operating temperatures and stresses in A-USC technology lies in the availability of appropriate materials with enhanced creep strength at intermediate temperature and with costs of manufacture and fabrication that will yield a cost of electricity acceptable to consumers [8]. The requirements imposed by these conditions are obviously beyond the temperature capacity of the presently widely used ferritic and austenitic steels for USC power plants, as steels are limited to temperature below 680 °C [5]. It is thus likely that nickel-based superalloys with higher temperature capacity will be needed, and some existing wrought Ni–Cr–Co-based superalloys such as IN740 [6], IN617 [5], Nimonic263 [9] are being evaluated as the candidate materials for USC. Despite of possessing excellent mechanical properties, they are all prohibitively expensive due to the addition of Co, Mo and W. Compared with those Ni-based superalloys, HR6W and GH2984 alloys have

Available online at <http://link.springer.com/journal/40195>

✉ Chuan-Yong Cui  
chycui@imr.ac.cn

<sup>1</sup> Institute of Metal Research, Chinese Academy of Sciences, Shenyang 110016, China

attracted much attention due to their low costs; however, it does not show high enough creep strength at high temperature of up to 700 °C. Therefore, a new superalloy with combination of low cost and enhanced strength beyond 700 °C has to be used. In present study, a new wrought Ni–Fe–Cr-based superalloy (named as HT700 alloy) with improved strength beyond 700 °C and with low cost was successfully developed.

## 2 Experimental

The nominal chemical compositions (wt%) of HT700 alloy are Ni-18Cr-2.8(W + Mo + Nb)-2.4Ti-1.8Al-0.15Si-0.5Mn-20Fe-0.06C-0.02P. The 1.8% Al in conjunction with 18% Cr is for the consideration of good oxidation resistance at high temperatures beyond 700 °C. Furthermore, the high contents of Al (1.8%) and Ti (2.4%) are expected to produce enough  $\gamma'$  precipitates which are beneficial to the creep strength and the yield strength. The additions of W and Mo are for the consideration of solid solution strengthening. The addition of 0.02% P is expected to increase the creep strength due to the enhancement of the grain boundary strength [10–14].

HT700 alloy was vacuum melted using high purity raw materials, homogenized at 1200 °C for 24 h and air-cooled. Then, the ingot was forged into block at 1160 °C. The HT700 alloy was aging heat treated at 750 °C for 16 h and then air-cooled. Tensile test specimens with 3 mm in gauge diameter and 15 mm in gauge length were machined from as-aged samples and tested in the temperature range from room temperature to 800 °C with a strain rate of  $3 \times 10^{-4} \text{ s}^{-1}$ . Tensile creep tests were carried on specimens with 5 mm in gauge diameter and 25 mm in gauge

length at various conditions. The microstructure was analyzed by scanning electron microscopy (SEM) equipped with EDS and transmission electron microscopy (TEM). The  $\gamma'$  was examined before and after creep-rupture test by SEM. Thermal-calc software, of which the database is TTNi7, was used to calculate theoretically the total volume fraction of  $\gamma'$  in HT700 alloy.

## 3 Results and Discussion

The microstructure of HT700 alloy is shown in Fig. 1. The microstructure mainly consisted of  $\gamma$  matrix, spherical  $\gamma'$  precipitates and carbides. Annealing twins in the  $\gamma$  grains were also observed. Carbides distributed at the grain boundaries and within the grains. Energy Dispersive Spectroscopy (EDS) analysis of the carbides identified the carbides formed within the grains mainly as MC type carbides, in which M is mostly substituted for Nb, Ti. The carbides observed at the grain boundaries are mainly  $M_{23}C_6$  type carbides in a form of ellipsoid (Fig. 1b), in which M is mainly substituted for Cr and Fe. Although 0.02 wt% of phosphorus is contained in HT700 alloy, no phosphide was observed both by SEM and by TEM. At higher magnification, spherical  $\gamma'$  particles within the grains were observed. The total volume fraction of the  $\gamma'$  in HT700 alloy was nearly 20% according to theoretical calculation based on thermal-calc software. The total volume fraction of the  $\gamma'$  in HT700 alloy is about 15% higher than that of GH2984 (about 6%), which might result in higher creep strength.

The tensile stress–strain curves of HT700 alloy at room temperature, 700, and 800 °C are shown in Fig. 2a. The tensile elongation of HT700 alloy at room temperature, 700, 800 °C was 16.3%, 15.5%, and 14.3%, respectively.

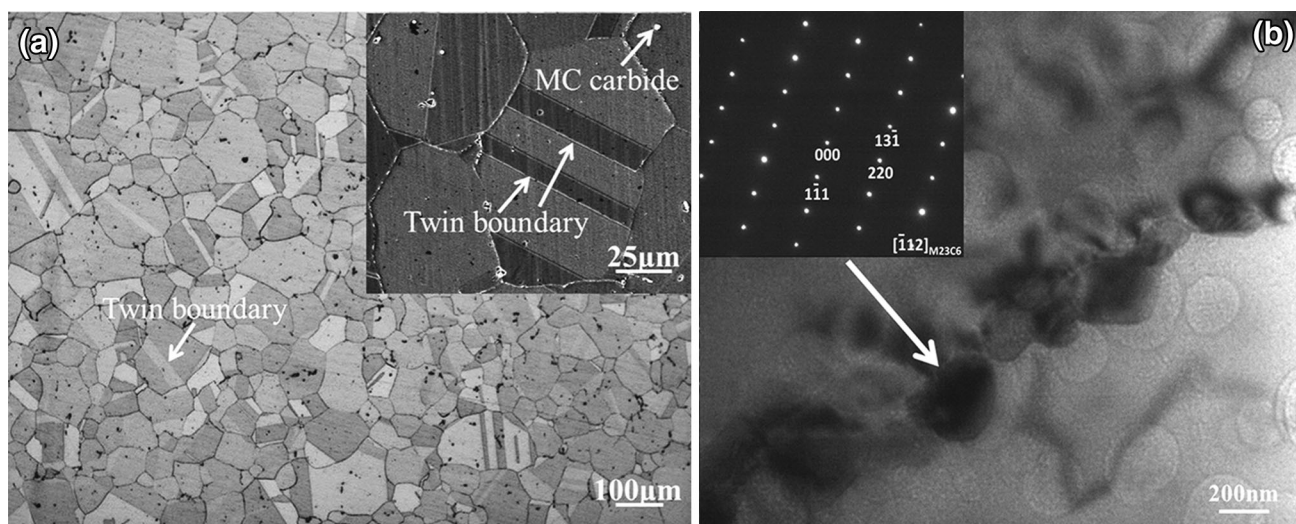


**Fig. 1** a Image of the HT700 alloy illustrating twin boundaries and MC carbides within the grains, b TEM morphology and SAED pattern of grain boundary precipitation

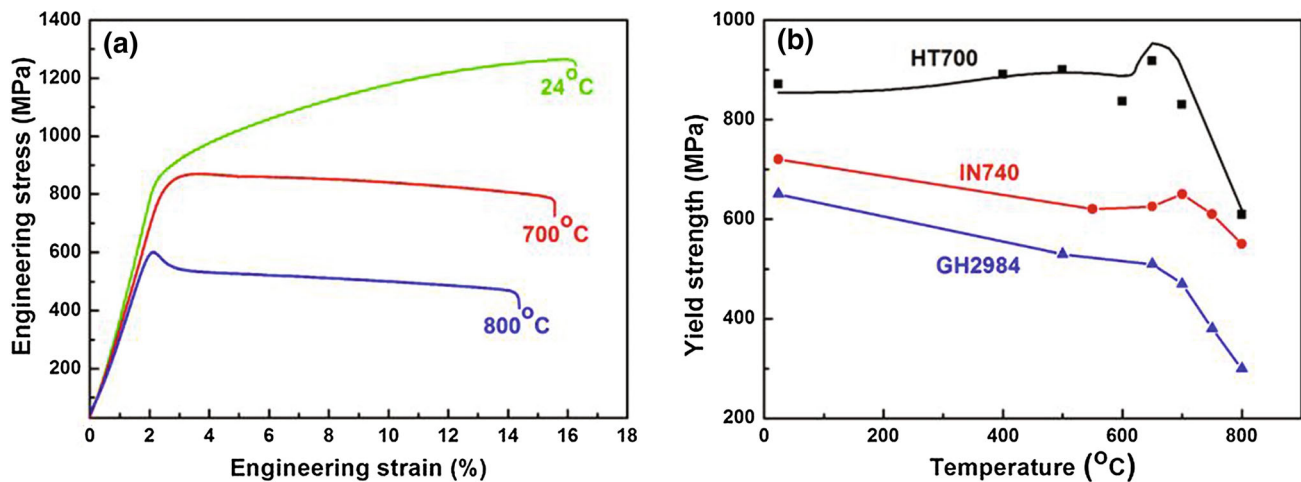


**Fig. 2** **a** Tensile engineering stress strain curves of HT700 alloy tested at room temperature, 700 and 800 °C, **b** comparison of tensile yield strength for HT700, IN740 and GH2984 alloys from room temperature to 800 °C

The ductility just had a mild decrease in the 700–800 °C range of interest and the tensile ductility at the temperature range from 700 to 800 °C was comparable to that at room temperature. The yield strength (YS) of HT700 alloy as a function of temperature is shown in Fig. 2b. The YS of IN740 and GH2984 alloys tested at different temperatures, which was obtained from Ref. [15], is also shown in Fig. 2b. The YS of HT700 alloy remained relatively constant at the temperature range from room temperature to 600 °C and even showed a small maximum at the temperatures in the vicinity of 650 °C and then decreased sharply with the temperature increasing. It is widely accepted that the flow stress of the  $\gamma'$  precipitates increases with the temperature increasing, but the  $\gamma'$  precipitates will soften when the temperature is high enough. Therefore, the relatively stable YS of HT700 alloy from room temperature to 600 °C could be explained based on the fact that the softening of  $\gamma$  matrix is compensated by the strengthening of  $\gamma'$  precipitates until about 600 °C. With temperature increasing further, strengthening of  $\gamma'$  precipitates is just partly offset by the softening of  $\gamma$  matrix and therefore the net effect will result in the YS of HT700 alloy increasing in the temperature range from 600 to 650 °C and even reaching the maximum at about 650 °C. However, sufficient thermal activation at high temperatures will lead to the softening of  $\gamma'$  precipitates and therefore the strength decrease in both  $\gamma$  matrix and  $\gamma'$  precipitates would result in the YS of HT700 alloy decreasing sharply in the temperature range from 650 to 800 °C. Compared with IN740 and GH2984 alloys, HT700 alloy had higher YS in the temperature range from room temperature to 800 °C. During 650–800 °C, the YS of HT700 alloy decreased sharply with the temperature increasing, resulting in the YS intervals between HT700 alloy and IN740 alloy to become increasingly narrow, but were still 300–400 MPa higher

than that of GH2984. This may be attributed to the fact that HT700 alloy has higher  $\gamma'$  content (about 20%) and finer grain size (56  $\mu\text{m}$ ) than that of GH2984 alloy. The microstructural parameters of GH2984 and IN740 were obtained from Refs. [6, 13, 16, 17], as shown in Table 1.

The fracture surfaces for the tensile tests subjected to different temperatures were examined by SEM. The fracture surfaces obtained at room temperature and 700 °C were selected to show the fracture transformation with test conditions changing, as shown in Fig. 3. Tensile specimen had a transgranular failure mode at room temperature, as clearly illustrated in Fig. 3a, b. The fracture surface obtained at 700 °C was similar to the fracture surface obtained at room temperature, but had a small portion of intergranular area on the edge of the tensile specimen. And secondary grain boundary cracking could be detected on the intergranular area, which demonstrates the grain boundary adhesion decreases when the temperature is high enough. It is worth noting that the intergranular area just occupied a small fraction of the entire fracture surface, demonstrating HT700 alloy still possesses relatively good grain boundary strength at 700 °C.

Creep curves of HT700 alloy tested at 750 °C and 200 MPa, at 750 °C and 250 MPa and at 800 °C and 200 MPa are shown in Fig. 4a. Creep curves tested at 750 °C and 250 MPa and at 800 °C and 200 MPa showed

**Table 1** Microstructural parameters of HT700, GH2984 and IN740 alloys

	Content of Al + Ti (wt.%)	Grain size ( $\mu\text{m}$ )	$\gamma'$ content (%)
HT700	4.2	56	20
GH2984	1.1–1.7	65	6
IN740	2.3–2.7	200	13

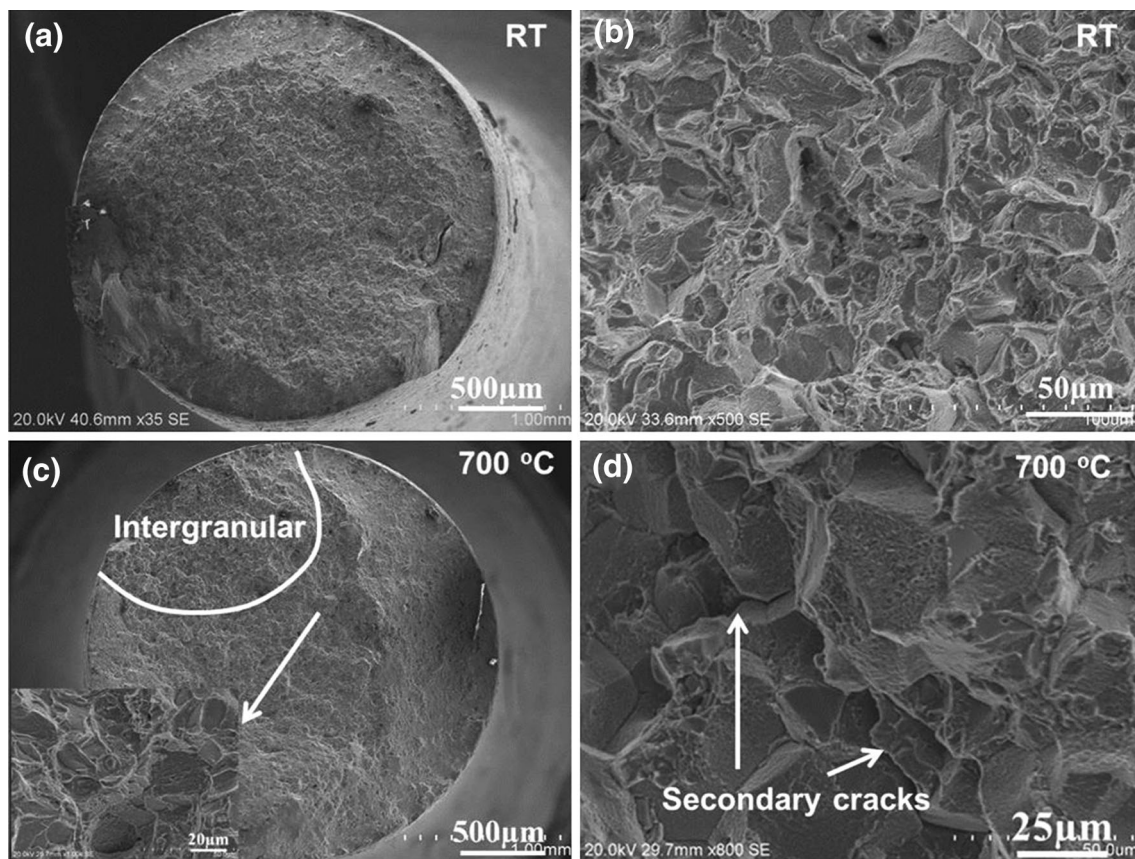


**Fig. 3** Typical fracture surfaces for tensile tests at room temperature **a, b**, 700 °C **c, d**. Note the fracture surface transformed from transgranular (room temperature) to predominantly transgranular but with small range intergranular area with grain boundary cracking

the same tendency with a short primary creep stage followed by a relatively little steady-state condition and then a very extended accelerating stage leading to failure. Creep curve tested at 750 °C and 200 MPa showed a relatively longer steady-state condition, and therefore creep-rupture

life at 750 °C and 200 MPa was longer (about 940 h). The Larson-Miller parameter (LMP) plot of GH2984 alloy which was obtained from Ref. [15] and that of HT700 are shown in Fig. 4b, which shows the creep resistance of HT700 alloy is much better than that of GH2984 alloy.

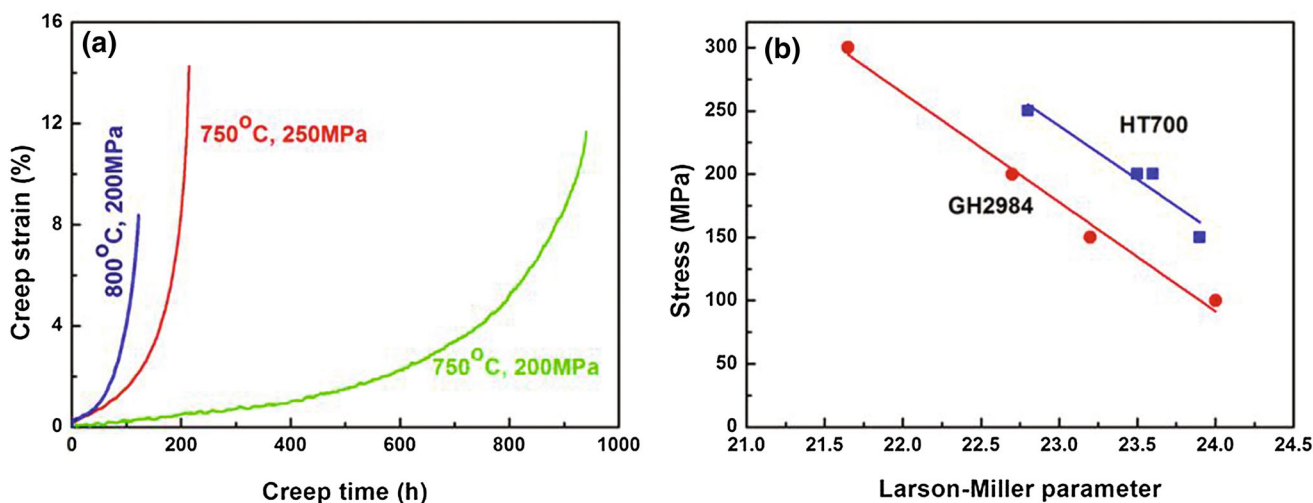


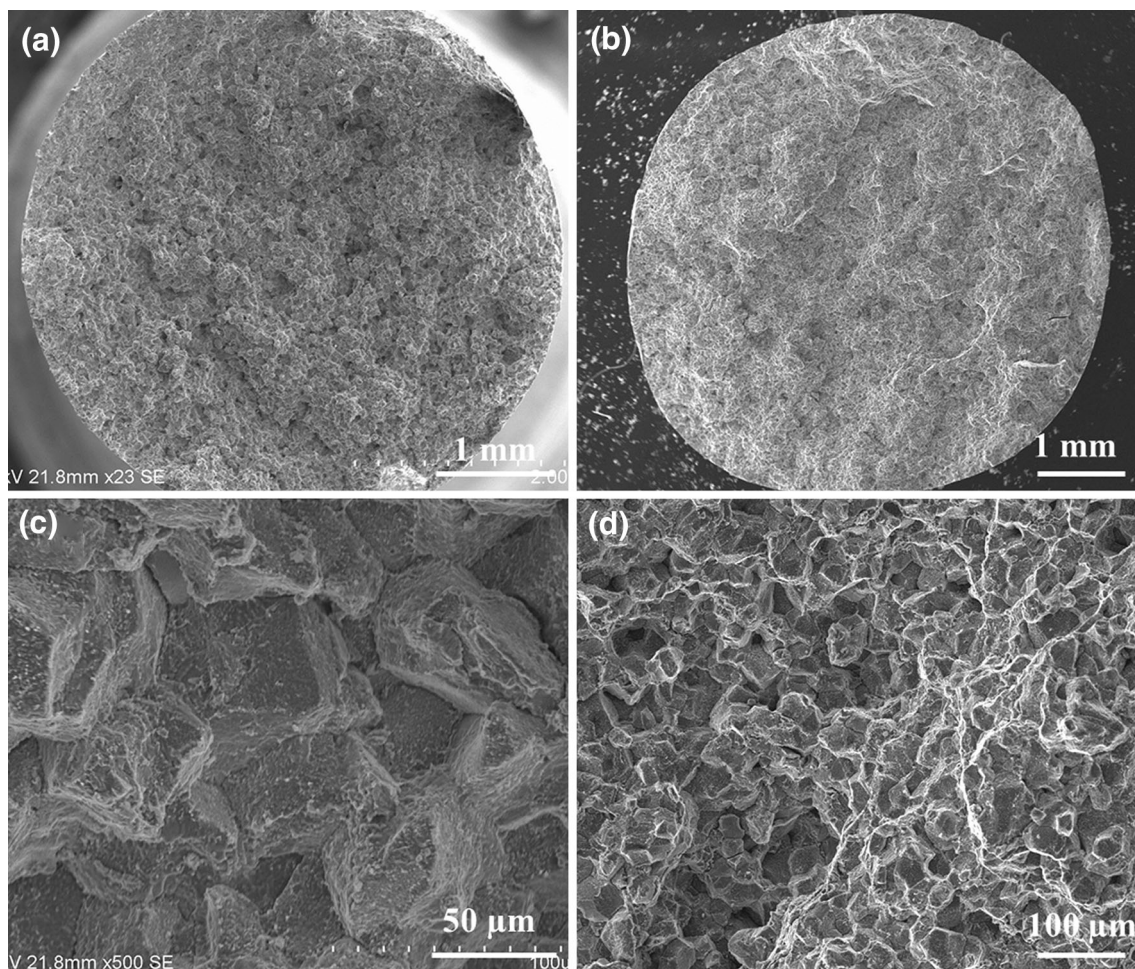
**Fig. 4** **a** Creep curves of HT700 alloy tested at 750 °C and 200 MPa, at 750 °C and 250 MPa and at 800 °C and 200 MPa; **b** LMP of HT700 alloy plotted as a function of stress, together with that of GH2984 alloy

**Table 2** Creep life and elongation of HT700 alloy tested at various conditions

Condition	Life (h)	Elongation (%)
750 °C/200 MPa	940	12
750 °C/250 MPa	215	16
800 °C/150 MPa	192	18
800 °C/200 MPa	122	10

Creep life and elongation of HT700 alloy tested at various conditions are listed in Table 2. Creep life decreased with increasing test temperature and applied stress level. For example, creep life of HT700 alloy decreased from 940 to 122 h when the temperature increased from 750 to 800 °C. At 750 °C, the creep life dropped from 940 to 215 h when the applied stress increased from 200 to 250 MPa. It is worth noting that creep-rupture life of HT700 alloy tested at 750 °C and 200 MPa was still two times longer than that of GH2984 alloy (444 h) tested at 750 °C and 150 MPa [15]. The longer creep-rupture life of HT700 alloy may be attributed to higher content of  $\gamma'$  (20%) and the addition of

trace P as grain boundary enhancement element. Although phosphorus has normally been regarded as a detrimental element in the cast superalloys, it draws attention in recent years that moderate addition of phosphorus as an alloying element could markedly prolong the creep life for some wrought superalloys such as GH761 [18, 19], IN718 [11, 12] and GH2984 [13]. Most researchers attributed the improvement in the creep life to the strengthened grain boundaries caused by phosphorus segregation on the grain boundaries which has already been confirmed by atom probe tomography [20]. So it is logical to deduce that phosphorus also segregates on the grain boundaries and strengthens the grain boundaries in HT700 alloy, thus prolonging the creep life of HT700 alloy. It must be also noted that HT700 alloy has relatively lower content of W (1 wt%) as compared with GH2984 alloy ( $\sim 2$  wt% W). W is generally regarded as a typical solid solution element and decreases the stacking fault energy (SFE) in the superalloys, thus improving creep properties of superalloys. Obviously, however, the decrease in creep life due to less W content in HT700 alloy is not able to contend with the

**Fig. 5** Typical fracture surfaces of the alloy crept at 750 °C/200 MPa **a, c**, 750 °C/250 MPa **b, d**

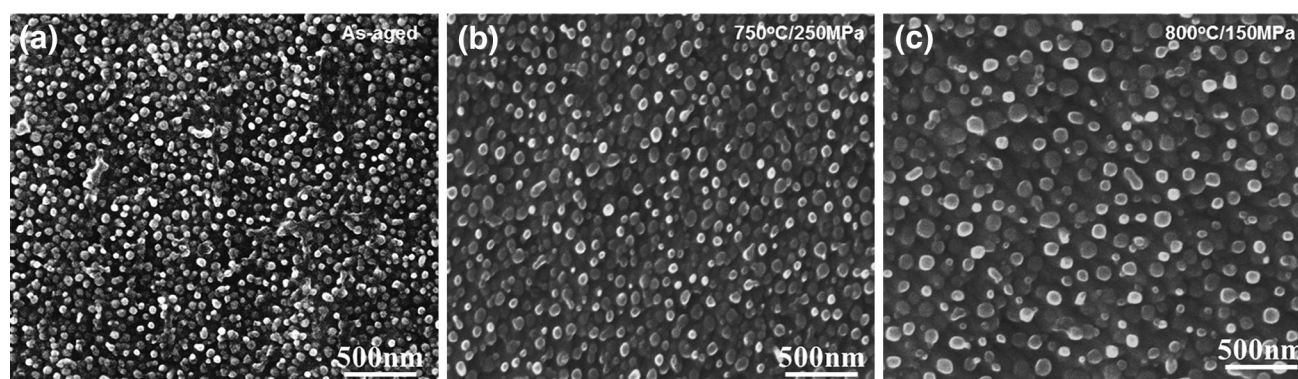


**Fig. 6** Typical  $\gamma'$  phase of as-aged HT700 alloy **a**, HT700 alloy **b** after creep rupture tested at 750 °C/250 MPa, **c** HT700 alloy after creep rupture tested at 800 °C/150 MPa

increase in creep life caused by higher volume fraction of  $\gamma'$  (20%) and the addition of trace P as grain boundary enhancement element.

Figure 5 shows typical creep fracture surfaces tested at 750 °C and 200 MPa and at 750 °C and 250 MPa. Creep specimens failed in an intergranular mode, which are different from tensile fracture mode. The appearance of fracture surface became rougher when the applied stress level increased, clearly shown in Fig. 5a and b, because the increased stress level would lead to more grain boundary cracks, thus leading to the linkage of cracks and consequently the fracture of the specimen.

The microstructure examinations of HT700 alloy before and after creep rupture by SEM showed that the  $\gamma'$  maintained its spherical morphology but coarsened during creep test. The size of  $\gamma'$  precipitates for as-aged HT700 alloy was less than 40 nm, however lots of  $\gamma'$  precipitates reached 70 nm after creep rupture tested at 750 °C and 250 MPa and 110 nm after creep rupture tested at 800 °C and 150 MPa, as shown in Fig. 6. The creep life of HT700 alloy tested at 750 °C and 250 MPa and at 800 °C and 150 MPa was 215 and 192 h, respectively. However, the size of  $\gamma'$  was much smaller after creep rupture tested at 750 °C and 250 MPa than that after creep rupture tested at 800 °C and 150 MPa, demonstrating HT700 alloy has more stable microstructural stability at 750 °C than at 800 °C.

#### 4 Summary

A newly developed HT700 alloy has higher yield strength than GH2984 and IN740 alloys from room temperature to 800 °C. The creep-rupture resistance of this new alloy is much better than that of the Ni–Fe-based superalloy GH2984 due to higher volume fraction of  $\gamma'$ . Good mechanical properties beyond 700 °C combined with low cost make this new superalloy appropriate for advanced ultra-supercritical power plant applications beyond 700 °C.

**Acknowledgments** This work was financially supported by the High Technology Research and Development Program of China (No. 2014AA041701) and the National Natural Science Foundation of China (Nos. 51171179, 51271174, 51331005, and 11332010).

#### References

- [1] R. Viswanathan, J.F. Henry, J. Tanzosh, G. Stanko, J. Shingledecker, B. Vitalis, R. Purgert, *J. Mater. Eng. Perform.* **14**, 281 (2005)
- [2] G. Stein-Brzozowska, D.M. Flórez, J. Maier, G. Scheffknecht, *Fuel* **108**, 521 (2013)
- [3] X.W. Cui, J.L. Hong, M.M. Cao, *Energy* **45**, 952 (2012)
- [4] P.D. Jablonski, J.A. Hawk, C.J. Cowen, P.J. Maziasz, *JOM* **64**, 271 (2012)
- [5] Q.Y. Wu, S. Hyojin, R.W. Swindeman, J.P. Shingledecker, V.K. Vasudevan, *Metall. Mater. Trans. A* **39**, 2569 (2008)
- [6] N.D. Evans, P.J. Maziasz, R.W. Swindeman, G.D. Smith, *Scr. Mater.* **51**, 503 (2004)
- [7] S.Q. Zhao, X.S. Xie, G.D. Smith, S.J. Patel, *Mater. Sci. Eng. A* **355**, 96 (2003)
- [8] T.B. Gibbons, *Trans. Indian Inst. Met.* **66**, 631 (2013)
- [9] M. Maldini, G. Angella, V. Lupinc, *Mater. Sci. Eng. A* **462**, 436 (2007)
- [10] N. Li, W.R. Sun, Y. Xu, S.R. Guo, D.Z. Lu, Z.Q. Hu, *Mater. Lett.* **60**, 17 (2006)
- [11] X.B. Liu, J.X. Dong, B. Tang, Y.H. Hu, X.S. Xie, *Mater. Sci. Eng. A* **270**, 190 (1999)
- [12] W.R. Sun, S.R. Guo, J.H. Lee, N.K. Park, Y.S. Yoo, S.J. Choe, Z.Q. Hu, *Mater. Sci. Eng. A* **247**, 173 (1998)
- [13] X. Xiao, H.Q. Zhao, C.S. Wang, Y.A. Guo, J.T. Guo, L.Z. Zhou, *Acta Metall. Sin.* **49**, 421 (2013). (in Chinese)
- [14] C.G. Mckamey, C.A. Carmichael, W.D. Cao, R.L. Kennedy, *Scr. Mater.* **38**, 485 (1998)
- [15] Z.H. Zhong, Y.F. Gu, Y. Yuan, Z. Shi, *Mater. Lett.* **109**, 38 (2013)
- [16] J.T. Guo, X.K. Du, *Acta Metall. Sin.* **41**, 1221 (2005). (in Chinese)
- [17] S.Q. Zhao, X.S. Xie, G.D. Smith, S.J. Patel, *Mater. Des.* **27**, 1120 (2006)
- [18] W.R. Sun, S.R. Guo, D.Z. Lu, Z.Q. Hu, *Metall. Mater. Trans. A* **28**, 649 (1997)
- [19] S.L. Yang, W.R. Sun, J.X. Wang, K.L. Wang, S.R. Guo, Z.Q. Hu, *Acta Metall. Sin.* **45**, 815 (2009). (in Chinese)
- [20] T. Alam, P.J. Felfer, M. Chaturvedi, L.T. Stephenson, M.R. Kilburn, J.M. Cairney, *Metall. Mater. Trans. A* **43**, 2183 (2012)